



## Updates on the Hard X-Ray Self-Seeding at the European XFEL

Shan Liu, Gianluca Geloni, Tianyun Long, Weilun Qin, Vitali Kocharyan, Jiawei Yan, Lu Cao, Naresh Kujala, Marc Guetg, Matthias Scholz & Winfried Decking

**To cite this article:** Shan Liu, Gianluca Geloni, Tianyun Long, Weilun Qin, Vitali Kocharyan, Jiawei Yan, Lu Cao, Naresh Kujala, Marc Guetg, Matthias Scholz & Winfried Decking (04 Apr 2025): Updates on the Hard X-Ray Self-Seeding at the European XFEL, Synchrotron Radiation News, DOI: [10.1080/08940886.2025.2472607](https://doi.org/10.1080/08940886.2025.2472607)

**To link to this article:** <https://doi.org/10.1080/08940886.2025.2472607>



© 2025 Deutsches Elektronen-Synchrotron DESY. Published with license by Taylor & Francis Group, LLC.



Published online: 04 Apr 2025.



Submit your article to this journal [↗](#)



Article views: 125



View related articles [↗](#)



View Crossmark data [↗](#)

# Updates on the Hard X-Ray Self-Seeding at the European XFEL

SHAN LIU,<sup>1</sup> GIANLUCA GELONI,<sup>2</sup> TIANYUN LONG,<sup>1</sup> WEILUN QIN,<sup>1</sup> VITALI KOCHARYAN,<sup>1</sup> JIAWEI YAN,<sup>2</sup> LU CAO,<sup>1</sup> NARESH KUJALA,<sup>2</sup> MARC GUETG,<sup>1</sup> MATTHIAS SCHOLZ,<sup>1</sup> AND WINFRIED DECKING<sup>1</sup>

<sup>1</sup>Deutsches Elektronen-Synchrotron DESY, Hamburg, Germany

<sup>2</sup>European XFEL, Schenefeld, Germany

## 1. Introduction

The European XFEL is a state-of-the-art hard X-ray free-electron laser (FEL) facility powered by a high-energy superconducting linear accelerator. Operating at megahertz repetition rates, it can deliver thousands of X-ray pulses per second within 10 Hz bursts, enabling unique opportunities for cutting-edge experiments [1]. At the European XFEL, FEL pulses are generated in the undulators through the Self-Amplified Spontaneous Emission (SASE) mechanism, which serves as the baseline mode of operation. The facility operates three beamlines: two dedicated to hard X-rays, SASE1 and SASE2, and one to soft X-rays, SASE3. Each hard X-ray beamline is equipped with 35 movable-gap, out-of-vacuum undulator cells. The SASE1 and SASE2 beamlines have achieved pulse energies of up to 5 mJ and 4 mJ at 9 keV, respectively, while SASE3 consistently delivers 8–10 mJ pulses at 1 keV, making the European XFEL a leader in high-intensity X-ray science. In pursuit of higher photon energy operations, significant milestones were reached in 2021. With a beam energy of 16.3 GeV, SASE1 demonstrated a pulse energy of 800  $\mu$ J at 24 keV, while SASE2 achieved a pulse energy of 340  $\mu$ J at 30 keV [2].

To achieve narrow bandwidth and high spectral brightness, a Hard X-ray Self-Seeding (HXRSS) system was installed at the SASE2 undulator beamline in 2019 and has been in user operation since 2021 [3,4]. Building on the successful implementation of HXRSS in SASE2, plans are underway to equip SASE1 with an HXRSS system by 2025. The European XFEL is the first facility to demonstrate HXRSS operation at MHz repetition rates in burst mode. To accommodate the high repetition rate, a cascaded two-stage monochromator design was implemented to minimize heat load on the crystal, particularly at photon energies below 8 keV [5]. Figure 1 illustrates the layout of the two-chicane HXRSS setup in the SASE2 beam line. This system can be used in different modes, in-

cluding the SASE mode (no chicane is used), one-chicane mode (only one of the two chicanes is used) and two-chicane mode (both chicanes are used). The design of the monochromator used at the European XFEL [6] is based on similar designs implemented at LCLS and PAL-XFEL.

Currently, the first monochromator has been removed due to radiation damage affecting the encoders of its movers. To address this issue, additional molybdenum shielding was added to the monochromators during the summer of 2024. The first monochromator is now reserved as a spare for replacement if needed. However, since the majority of users require photon energies above 7 keV, this issue has not impacted user operations.

## 2. Operation and user delivery highlights

The SASE2 beamline supports two instruments: MID, dedicated to materials imaging and dynamics, and HED, focused on high-energy density science. Since the introduction of the HXRSS system in 2021, user demand for HXRSS capabilities has steadily increased, with nearly 50% of user requests in 2024 involving HXRSS. Figure 2 illustrates the performance statistics of the HXRSS system from 2021 to 2024. Performance variations over time reflect changes in machine status and optimization efforts. The system has achieved a total pulse energy of up to 1.4 mJ, with an average intensity of 500  $\mu$ J. Within the seeded bandwidth (BW), pulse energies range between 400–1,000  $\mu$ J at 6–10 keV and 150–400  $\mu$ J at 10–17 keV. Figure 3 shows the user delivery at 9 keV with a total pulse energy of up to 1.4 mJ and a background of 400  $\mu$ J. The spectral density reached above 1 mJ/eV. The generated X-ray pulse is characterized by the XGM pulse energy monitor [7] and the HIREX single shot spectrometer [8], located in the photon beam transport approximately 500 m downstream of the undulator.

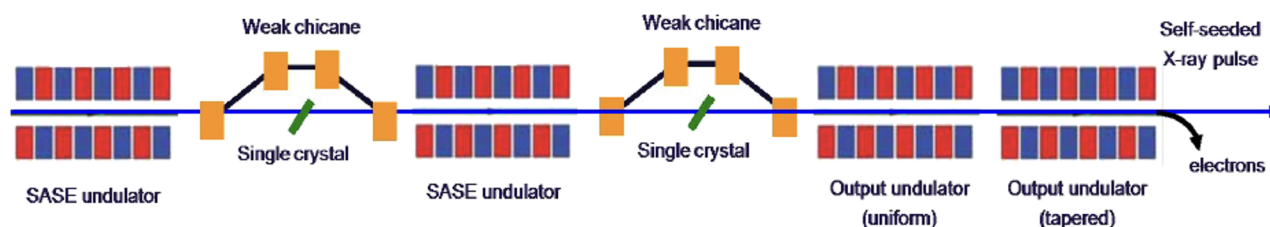


Figure 1: Layout of the cascaded HXRSS setup at the SASE2 undulator of European XFEL.

© 2025 Deutsches Elektronen-Synchrotron DESY. Published with license by Taylor & Francis Group, LLC.

This is an Open Access article distributed under the terms of the Creative Commons Attribution License (<http://creativecommons.org/licenses/by/4.0/>), which permits unrestricted use, distribution, and reproduction in any medium, provided the original work is properly cited. The terms on which this article has been published allow the posting of the Accepted Manuscript in a repository by the author(s) or with their consent.



Figure 2: HXRSS performance statistics from 2021 to 2024. The upper plot shows the total pulse energy (blue) and SASE BG (orange); the middle plot shows the percentage of pulse energy in seeding (blue) and in SASE BG (orange); the lower plot shows the bandwidth of the seeded spectra. Please note that different users may have different requests on seeding pulse energy and bandwidth.

Effective HXRSS operation requires precise alignment of the undulators, ensuring sufficient contributions to lasing from cells both upstream and downstream of the monochromator. However, achieving optimal alignment in the SASE2 beamline is particularly challenging, as the first and last cells often contribute less effectively to lasing. In most setups, the second monochromator alone is used to ensure at least 30  $\mu\text{J}$  of energy reaches the crystal. At higher photon energies, maximizing the contribution of downstream undulator cells to the amplification of the HXRSS signal is crucial.

Recently, significant improvements were achieved by combining electron beam-based alignment (BBA) [9, 10] with photon beam-based

alignment [11], and employing “sliding window” optimization in the linear regime. These strategies have enhanced alignment precision and lasing performance.

For bandwidth and signal-to-noise ratio (SNR) control, the spectral bandwidth of the HXRSS system has been shown to strongly depend on the electron beam energy profile [12]. Both simulations and experiments have demonstrated shifts in the central photon energy with linear energy chirps, as well as bandwidth broadening with nonlinear energy chirps during the seeding amplification process. Notably, experiments and simulations indicate that asymmetric current profiles with peak current positioned at the beam head are advantageous. An example of longitudinal phase space measured using the corrugated structure installed downstream of the SASE2 beamline is shown in Figure 4 [13]. By fine-tuning parameters such as chirp, curvature, skewness, and the first- and second-order terms of inverse global compression, a desirable beam profile with peak current favorably located at the head can be achieved. This minimizes energy chirp within the lasing window, resulting in narrower bandwidth and improved SNR. Additionally, background control has been enhanced by utilizing different tapering profiles, which are now frequently employed during user deliveries to optimize performance.

In the experiment, the background level can be measured by either extracting the crystal or slightly detuning its pitch angle to disrupt the seeding condition. A record-low background level of less than 4% was achieved at 11 keV, with a total pulse energy of approximately 600  $\mu\text{J}$  and a background contribution of less than 20  $\mu\text{J}$ , which is close to the noise threshold of the XGM (see Figure 5).

Meanwhile, we are exploring additional approaches to further reduce the spectral bandwidth. These include establishing a longer lasing window through high-charge operation modes and utilizing higher-index reflections, as demonstrated at PAL-XFEL [14].

As in the SASE delivery mode, 9 keV is the photon energy requested most by the users for HXRSS. However, higher seeded photon energies are increasing in demand for advanced experiments. The European XFEL is currently the only facility capable of providing HXRSS at photon energies above 15 keV. The main challenges in achieving higher photon energies are ensuring sufficient energy impinges on the crystal and effectively amplifying the seeded signal after the monochromator.

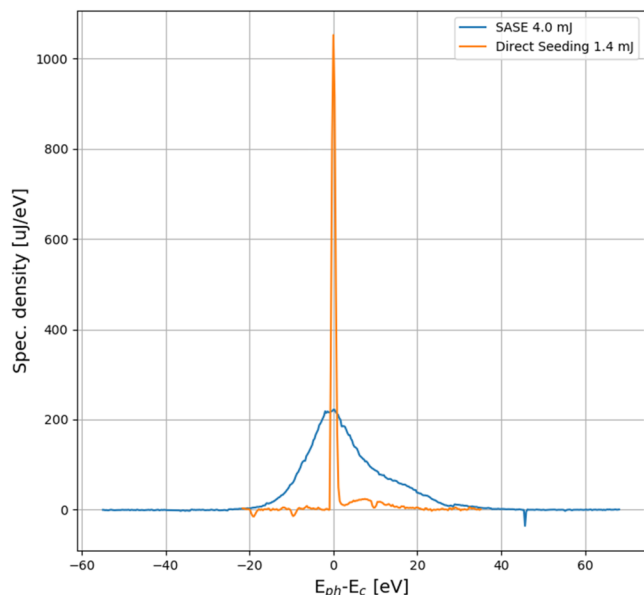


Figure 3: HXRSS performance at 9 keV during a user delivery in 2024. The total seeded pulse energy reached approximately 1.4 mJ, with a background contribution from SASE of around 400  $\mu\text{J}$ . The average spectral density exceeded 1 mJ/eV, calculated over 1,000 shots. Prior to seeding, the SASE was tuned to approximately 4 mJ at 8.5 keV. During the 4-week continuous seeding delivery campaign, no additional SASE tuning was conducted at 9 keV. The transition from 8.5 keV to 9 keV was achieved directly under seeding conditions.

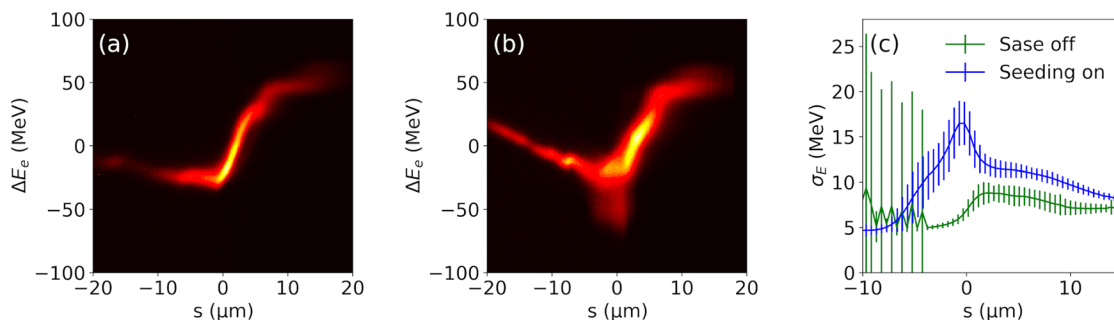


Figure 4: Electron beam analysis. Reconstructed longitudinal phase space from passive streaker measurements with Curvature1 for SASE off (a) and seeding on (b). (c) slice energy spread.

Leveraging the long undulator beamlines and the cascaded setup, the monochromator in the second chicane was used to achieve seeding at 18 keV. The first successful demonstration of seeding at 18 keV achieved a spectral density exceeding  $150 \mu\text{J}/\text{eV}$ , as shown in Figure 6 (left). At the end of 2024, we successfully delivered HXRSS at 17 keV with a total pulse energy of 180  $\mu\text{J}$  and an average spectral density of approximately  $140 \mu\text{J}/\text{eV}$ —more than twice the average spectral den-

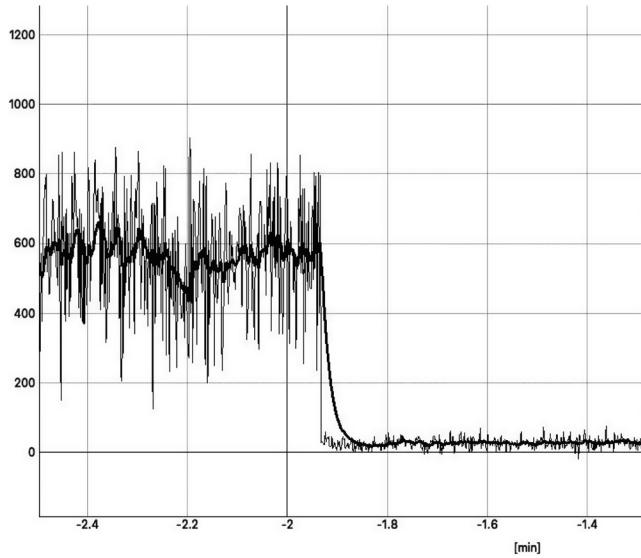


Figure 5: Pulse energy in  $\mu\text{J}$  measured by XGM with seeding at 11 keV, the measured pulse energy before (total pulse energy) and after (SASE background) retracting the crystal were 600  $\mu\text{J}$  and 20  $\mu\text{J}$ , respectively.

sity achieved with 1.3 mJ SASE pulses, as shown in Figure 6 (right). The spectral full width at half maximum (FWHM) was around 0.7 eV.

The combination of high repetition rates, elevated spectral density, and the capability to perform energy scans enables groundbreaking experiments. For instance, an exceptionally narrow nuclear resonance was detected in  $^{45}\text{Sc}$  [15]. To facilitate such studies, a dedicated HXRSS tool has been developed, allowing users to directly control the HXRSS wavelength and execute precision scans. Figure 7 (left) illustrates an example of such scans conducted during the nuclear resonance experiments. In October 2024, another user run was delivered for nuclear resonance studies, this time with significantly higher spectral density, as shown in Figure 7 (right). Results from these experiments are expected to be reported in the near future.

### 3. Investigation of advanced HXRSS operation modes

To further enhance the flexibility and tunability of HXRSS, several advanced operation schemes are currently being explored at the European XFEL. These include two-color HXRSS, second harmonic generation, and phase-locked HXRSS.

Two-color HXRSS can be achieved by utilizing two crystal reflection lines that lie adjacent to each other within the SASE bandwidth. These two lines can be generated by a non-zero raw angle, the concept of which was first demonstrated at LCLS [16]. One can also seed near the crossing of two reflections, in this case, the energy separation of the two colors can be tuned by adjusting the crystal's pitch angle. At the European XFEL, two-color HXRSS was successfully delivered to the MID instrument for the commissioning of the split-and-delay line. This system enables two-color operation with a delay range from  $-10$  to  $800 \text{ ps}$  [17]. Such a scheme is particularly valuable for user experiments

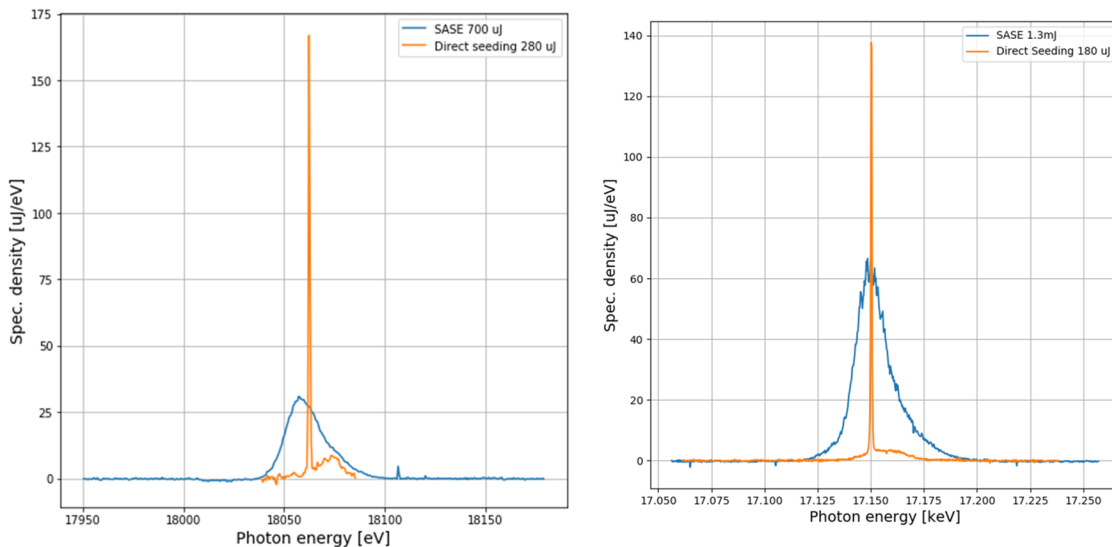


Figure 6: Demonstration of seeding at 18 keV (left) and user delivery of 17 keV (right) compared with the SASE level tuned before setting up seeding. The spectra shown are averaged over 1,000 shots.

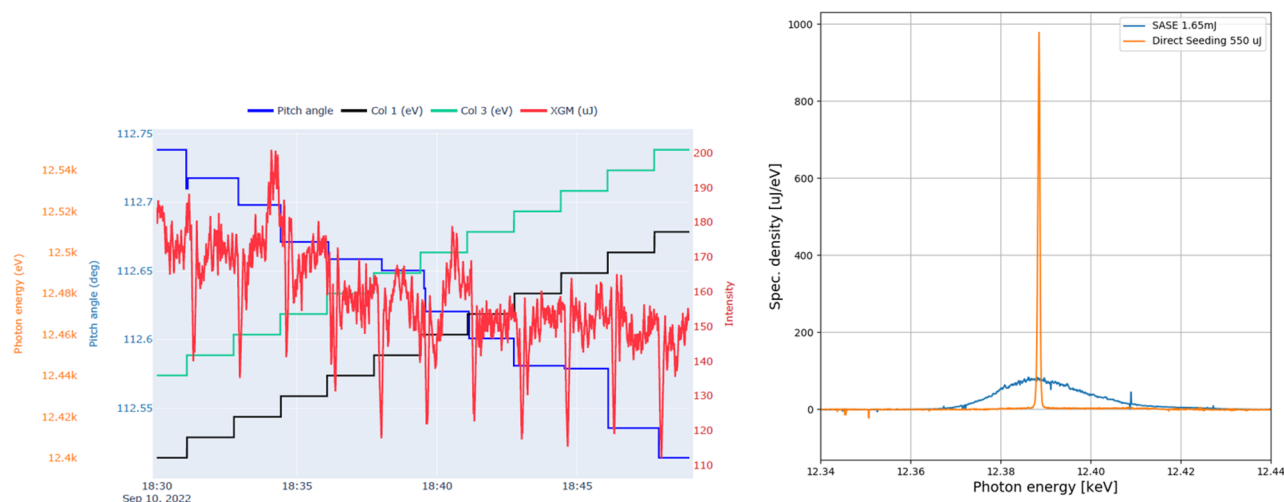


Figure 7: Seeding photon energy scans by changing the pitch angle during the first user delivery for 45Sc experiment (left), spectral density (averaged over 1,000 shots) reached during 2<sup>nd</sup> user delivery for 45Sc experiment compared with the SASE level tuned before setting up seeding (right).

requiring variable delays between two photon energies, especially for pump-probe experiments.

The combination of HXRSS with a second harmonic generation scheme for producing seeded signals at higher photon energies was proposed in [18]. This approach has been demonstrated at the European XFEL across various photon energies, including transitions from a 7.5 keV fundamental to a 15 keV second harmonic and from a 9 keV fundamental to an 18 keV second harmonic. In this scheme, the undulator section downstream of the monochromator is divided into two parts. The first section amplifies the seeded signal at the fundamental wavelength, while the second section is configured to resonate at the second harmonic. The bunching of second harmonic generated by the upstream seeding process at the fundamental wavelength is then utilized to produce a seeded signal at the second harmonic, enabling higher photon energy output with improved spectral properties.

The main challenge of this scheme is achieving sufficient amplification of the second harmonic with the limited number of undulator cells available downstream. In our case, up to five cells contributed to the amplification. However, improved alignment of the remaining cells can help to achieve higher pulse energy, as previously mentioned. Another significant challenge is accurately characterizing the pulse energy of the second harmonic, as the XGM exhibits substantial contamination from the fundamental wavelength, even when operated in higher photon energy mode.

To address this, we first calibrated the HIREX diagnostic using XGM under 18 keV SASE conditions. The calibrated HIREX signal was then used to estimate the pulse energy of the second harmonic, which was determined to be approximately 7  $\mu$ J. Please note that, in this measurement, there were only three cells contributing to the amplification. Additionally, the use of a diamond sensor [19] installed downstream of SASE2 is being investigated as a potential diagnostic tool for measuring the second harmonic.

Phase-locked HXRSS was investigated as a means to enable coherent control experiments. Theoretical analyses and start-to-end simulations have been conducted for generating phase-locked pulses using the HXRSS system at the European XFEL [20]. Inspired by the method proposed in Ref. [21], which combines self-seeding with fresh-slice lasing techniques, our approach exploits different transverse centroid offsets along the electron beam, taking advantage of the CSR effect in the distribution arc of the SASE2 beamline. In this scheme, a portion of the electron beam is first used to produce SASE radiation, which is then filtered and utilized as a seed. Subsequently, HXRSS pulses are generated from other parts of the beam by applying appropriate transverse kicks. The resulting radiation consists of coherent pulses with a fixed phase difference and a tunable time delay within the bunch length. This technique holds significant potential for applications such as coherent X-ray pump-probe experiments, enabling precise temporal and phase control.

#### 4. Summary and future plans

The HXRSS system at the European XFEL offers researchers unprecedented opportunities in experiments requiring high-brightness, monochromatic X-ray beams. The photon energy range currently explored spans from 6 to 18 keV. Its unique cascaded design can not only effectively handle the head load issue at photon energies below 8 keV but also increase the SNR of the output signal. At photon energies above 8 keV, the heat-load effect has been shown to be negligible. Notably, at 9 keV, the system achieved an average spectral density exceeding 1 mJ/eV, corresponding to approximately 4 W/eV of X-ray average power density with 4,000 bunches per second. Successful seeding at 18 keV has also been demonstrated, yielding a spectral density of 150  $\mu$ J/eV, which significantly exceeds the performance of millijoule-level SASE pulses.



Several advanced operational modes, including two-color HXRSS, second harmonic generation, and phase-locked HXRSS, have been investigated and are under further development.

The HXRSS system's ability to combine high repetition rates with exceptional spectral density has enabled groundbreaking experiments and met the growing demand for its unique capabilities. Future development efforts will focus on enhancing performance through refinements in bandwidth and background control. Advanced techniques, such as longitudinal phase space manipulation and the implementation of specialized taper profiles, are being explored to further optimize X-ray beam quality and stability. These efforts aim to ensure continued innovation and address the evolving needs of the scientific community.

### Disclosure statement

No potential conflict of interest was reported by the authors. ■

### References

1. W. Decking et al., *Nat. Photonics* **14** (6), 391 (2020). doi:[10.1038/s41566-020-0607-z](https://doi.org/10.1038/s41566-020-0607-z)
2. Y. Chen et al., *J. Phys: Conf. Ser.* **2420** (1), 012026 IOP Publishing, (2023). doi:[10.1088/1742-6596/2420/1/012026](https://doi.org/10.1088/1742-6596/2420/1/012026)
3. G. Geloni, V. Kocharyan, and E. Saldin, *J. Mod. Opt.* **58** (16), 1391 (2011). doi:[10.1080/09500340.2011.586473](https://doi.org/10.1080/09500340.2011.586473)
4. S. Liu et al., *Phys. Rev. Accel. Beams* **22** (6), 060704 (2019). doi:[10.1103/PhysRevAccelBeams.22.060704](https://doi.org/10.1103/PhysRevAccelBeams.22.060704)
5. S. Liu et al., *Nat. Photon.* **17** (11), 984 (2023). doi:[10.1038/s41566-023-01305-x](https://doi.org/10.1038/s41566-023-01305-x)
6. L. Samoylova et al., *AIP Conference Proceedings*, 2019. Vol. 2054. No. 1. AIP Publishing.
7. T. Maltezopoulos et al., *J. Synchrotron Rad.* **26** (4), 1045 (2019). doi:[10.1107/S1600577519003795](https://doi.org/10.1107/S1600577519003795)
8. N. Kujala et al., *Rev. Sci. Instrum.* **91** (10), 103101 (2020). doi:[10.1063/5.0019935](https://doi.org/10.1063/5.0019935)
9. P. Emma, R. Carr, and H.-D. Nuhn, *Nucl. Instrum. Methods Phys. Res., Sect. A* **429**, 407 (1999) **429** (1-3), 407 (1999). doi:[10.1016/S0168-9002\(99\)00117-5](https://doi.org/10.1016/S0168-9002(99)00117-5)
10. M. Scholz, W. Decking, and Y. Li, *Proc. FEL'19*, 592 (2019).
11. T. Tanaka et al., *Phys. Rev. Special Topic Accelerat Beam.* **15** (11), 110701 (2012).
12. T. Long et al., Control of bandwidth and signal-to-noise ratio for hard-X-ray self-seeded free-electron lasers, *Phys. Rev. Appl.* Accepted 25 March 2025.
13. P. Dijkstal, W. Qin, and S. Tomin, *Phys. Rev. Accel. Beams* **27** (5), 050702 (2024). doi:[10.1103/PhysRevAccelBeams.27.050702](https://doi.org/10.1103/PhysRevAccelBeams.27.050702)
14. I. Nam et al., *Nat. Photonics* **15** (6), 435 (2021). doi:[10.1038/s41566-021-00777-z](https://doi.org/10.1038/s41566-021-00777-z)
15. Y. Shvyd'ko et al., *Nature* **622** (7983), 471 (2023). doi:[10.1038/s41586-023-06491-w](https://doi.org/10.1038/s41586-023-06491-w)
16. A. A. Lutman et al., *Phys. Rev. Lett.* **113** (25), 254801 (2014). doi:[10.1103/PhysRevLett.113.254801](https://doi.org/10.1103/PhysRevLett.113.254801)
17. W. Lu et al., Compact EUV & X-ray Light Sources, 2022, pp. JTh4A-11. Optica Publishing Group, doi:[10.1364/EUVXRAY.2022.JTh4A.11](https://doi.org/10.1364/EUVXRAY.2022.JTh4A.11)
18. G. Geloni et al., Scheme to increase the output average spectral flux of the European XFEL at 14.4 keV, <https://arxiv.org/pdf/1508.04339>.
19. T. Çonka Yıldız et al., *Synchrotron Radiation* **31** (5) 1029 (2024). doi:[10.1107/S1600577524006015](https://doi.org/10.1107/S1600577524006015)
20. T. Long et al., Phase-Locked Hard X-Ray Self-Seeding FEL Study for the European XFEL, *Proc. FEL'22*, 246 (2022). doi:[10.18429/JACoW-FEL2022-TUP44](https://doi.org/10.18429/JACoW-FEL2022-TUP44)
21. S. Reiche et al., *Proc. Natl. Acad. Sci. USA.* **119** (7), e2117906119 (2022). doi:[10.1073/pnas.2117906119](https://doi.org/10.1073/pnas.2117906119)